

BCcI, the novel antineoplastic nanocomplex, showed potent anticancer effects in vitro and in vivo

Somayah Kalanaky^{1,2}
 Maryam Hafizi¹⁻³
 Saideh Fakharzadeh¹
 Mohammad Vasei⁴
 Ladan Langroudi⁵
 Ehsan Janzamin⁶
 Seyed Mahmoud Hashemi⁷
 Maryam Khayamzadeh²
 Masoud Soleimani⁶
 Mohammad Esmaeil Akbari²
 Mohammad Hassan Nazaran¹

¹Department of Research and Development, Sodour Ahrar Shargh Company, Tehran, Iran; ²Cancer Research Centre, Shahid Beheshti University of Medical Sciences, Tehran, Iran; ³Stem Cell Technology Research Center, Tehran, Iran; ⁴Department of Pathology, Tehran University of Medical Sciences, Tehran, Iran; ⁵Department of Immunology, Faculty of Medical Sciences, Tarbiat Modares University, Tehran, Iran; ⁶Department of Haematology, Faculty of Medical Sciences, Tarbiat Modares University, Tehran, Iran; ⁷Department of Immunology, Faculty of Medicine, Shahid Beheshti University of Medical Sciences, Tehran, Iran

Correspondence: Mohammad Esmaeil Akbari
 Cancer Research Center, Shahid Beheshti University of Medical Sciences, Tehran, Iran
 Tel +98 21 2272 4090
 Fax +98 21 2274 9213
 Email crcsbmu@gmail.com

Mohammad Hassan Nazaran
 Department of Research and Development, Sodour Ahrar Shargh Co., Tehran, Iran
 Tel +98 21 8899 2123
 Fax +98 21 8895 3212
 Email mnazaran@nanochelatingtechnology.com

Purpose: In spite of all the efforts and researches on anticancer therapeutics, an absolute treatment is still a myth. Therefore, it is necessary to utilize novel technologies in order to synthesize smart multifunctional structures. In this study, for the first time, we have evaluated the anticancer effects of BCcI nanocomplex by vitro and in vivo studies, which is designed based on the novel nanochelating technology.

Methods: Human breast adenocarcinoma cell line (MCF-7) and mouse embryonic fibroblasts were used for the in vitro study. Antioxidant potential, cell toxicity, apoptosis induction, and CD44 and CD24 protein expression were evaluated after treatment of cells with different concentrations of BCcI nanocomplex. For the in vivo study, mammary tumor-bearing female Balb/c mice were treated with different doses of BCcI and their effects on tumor growth rate and survival were evaluated.

Results: BCcI decreased CD44 protein expression and increased CD24 protein expression. It induced MCF-7 cell apoptosis but at the same concentrations did not have negative effects on mouse embryonic fibroblasts viability and protected them against oxidative stress. Treatment with nanocomplex increased survival and reduced the tumor size growth in breast cancer-bearing balb/c mice.

Conclusion: These results demonstrate that BCcI has the capacity to be assessed as a new anti-cancer agent in complementary studies.

Keywords: BCcI, cancer, nanotechnology, nanochelating technology, nanocomplex

Introduction

According to the World Health Organization reports, the mortality associated with cancer will be increased from 7.4 million in 2004 to 11.8 million by 2030.¹ The currently used therapies are surgery, radiotherapy, and chemotherapy. The chemotherapy agents nonselectively have severe adverse effects on healthy tissues.^{2,3} These drugs have limited mechanism of actions and target one or two signaling pathways, and so cancer cells are able to evade chemotherapy agents and escape from being killed by selective resistance pathways.⁴ Therefore, more tumor-selective approaches and targeting neoplastic cells via various pathways may be necessary in designing new anticancer drugs.

In the recent decades, medical researchers have highly regarded using nanotechnology to improve the effectiveness of medicines. Owing to the special nature of cancer cells and the requirement of selective drug functions protecting healthy cells to remain safe from side effects, this technology can be used in the pharmaceutical industry to increase the selectivity and to enhance drug performances.⁵ Currently, much of the focus on the use of nanotechnology in medical science is in the anti-cancer drug innovation field.⁶ The nanotechnology-based drug delivery systems have many advantages as a potent platform for anticancer therapy, such as improved drug availability, high drug loading efficiency, resistance to recrystallization upon

encapsulation, and spatially and temporally controllable drug releases.⁷ However, several obstacles, including difficulty in achieving the optimal combination of physicochemical parameters for tumor targeting, evading particle clearance mechanisms, and controlling drug releases, prevent the translation of nanomedicines into therapy.⁸ Hence, efforts have been focused on developing safer and more efficient nanotechnology-based structures.

For the first time, we have synthesized BCc1 nanocomplex based on the novel nanochelating technology by a self-assembly method and evaluated its anticancer effects. In this study, we have assessed the “therapeutic behavior” potential of BCc1 by *in vitro* and *in vivo* studies.

In the previous studies, which used modern nanochelating technology, we synthesized Hep-c,⁹ MSc1, Pac, Pas, and Paf nanocomplexes. The first nanocomplex Hep-c improved cellular immunity responses against hepatitis B vaccine.

In another study, MSc1 nanocomplex showed therapeutic behavior in an animal model of multiple sclerosis and prevented H₂O₂-induced cell death even after binding with iron in an *in vitro* model of oxidative stress.¹⁰ Also Pac, Pas, and Paf nanocomplexes showed neuroprotective effects in the cellular model of Parkinson’s disease.¹¹

Many studies have shown the determinant role of iron metabolism in cancer pathogenesis.^{12,13} The iron-dependent ribonucleotide reductase is the rate-limiting enzyme in DNA synthesis and considers the requirements of proliferating cells. Therefore, cancer cells are more dependent on the concentrations of iron.¹⁴ The research has shown that iron chelators inhibit ribonucleotide reductase and cyclin-dependent kinase activity, and thus, the cell cycle arrests in the G1 phase.¹⁵ These structures induce N-myc downstream-regulated gene 1 (NDRG1) expression, which in turn inhibits growth, angiogenesis, and metastasis of malignant cells.^{16–19} So, one important feature of BCc1 is its chelating property, and the dominant affinity of this nanocomplex is for iron.

CD44 and CD24 are the most consistently used biomarkers to identify and characterize the breast cancer stem cells’ phenotype.²⁰ CD44 has been shown to promote protumorigenic signaling and advance the metastatic cascade.²¹ So, in this study, BCc1 potential to affect the expression of these markers was evaluated.

Available reports imply that oxidative stress has an important role in the pathogenesis of cancer and its progression.^{22,23} One of the common models for mimicking the oxidative stress *in vitro* is using H₂O₂ as a free radical source.²⁴ Thus, we used this common cellular model to evaluate the effect of BCc1 on preventing oxidative stress-associated cell death.

Materials and methods

BCc1 was synthesized by Sodour Ahrar Shargh Co. (Tehran, Iran). Hydrogen peroxide (H₂O₂), sodium isothiocyanate, dimethyl sulfoxide, FeCl₃, nitric acid, acetone, methanol, and formalin were purchased from EMD Millipore (Billerica, MA, USA). Dulbecco’s Modified Eagle’s Medium, RPMI-1640, fetal bovine serum, penicillin G and streptomycin (100 µg/mL), and 0.25% trypsin–ethylenediaminetetraacetic acid (EDTA) were purchased from Thermo Fisher Scientific (Waltham, MA, USA). Hematoxylin and eosin (H&E) and 99% 3-(4,5-dimethylthiazol-2-yl)-2,5-diphenyltetrazolium bromide (MTT) were acquired from Sigma-Aldrich Co. (St Louis, MO, USA). All antibodies, annexin V, and propidium iodide were obtained from BD Biosciences (San Jose, CA, USA).

The list of the equipments and instruments used is as follows: electrical conductance meter and pH meter BEM802 (Milwaukee, Italy), rheometer (Brookfield Engineering Laboratories, Inc., Middleboro, MA, USA), atomic absorption spectrometer (2100; PerkinElmer Inc., Waltham, MA, USA), transmission electron microscope (CM-200 FEG; FEI company, Hillsboro, OR, USA), scanning electron microscopy (VEGA-TESCAN-LMU; TESCAN, Czech Republic), spectrum two infrared (IR) spectrometers (L160000A, PerkinElmer Inc., Waltham, MA, USA), absorbance microplate readers (ELx800; Winooski, VT, USA), B51 microscope and DP72 camera (Olympus Corporation, Tokyo, Japan), automated blood analyzer (XS 800i; Sysmex, USA), FACSCalibur cytometer (BD Biosciences, San Jose, CA, USA), and light microscope (Axio Scope.A1; Zeiss, Germany).

Cell culture

Human breast adenocarcinoma cell line (MCF-7) and mouse embryonic fibroblasts (MEFs) were purchased from the National Cell Bank of Pasteur Institute (Tehran, Iran) and were cultured in Dulbecco’s Modified Eagle’s Medium supplemented with 10% fetal bovine serum and penicillin G and streptomycin (100 µg/mL). Cells were cultured under humidified atmosphere of 95% air, with 5% CO₂ at 37°C in a 25 cm² culture flask. Cancer Research Center, Shahid Beheshti University of Medical Sciences Institutional Review board does not require review for human cell lines.

Animals

Six-to-eight-week-old inbred female BALB/c mice were purchased from Pasteur Institute, Tehran, Iran. All the animal studies were approved by the Tehran University of Medical Sciences. All mice were maintained in large group houses under 12-hour dark/light cycles with proper access to food and water.

Synthesis and characterization of BCc1

Nanochelating technology was used by the Sodour Ahrar Shargh Co. to design and synthesize the BCc1 nanocomplex.²⁵ The synthesis of poly organic acid was done in a typical procedure: 30.2 g organic acid, 10.40 mL ethanol, and 100 mL deionized water were added to a 250 mL three-neck round-bottom flask fitted with an inlet adapter and an outlet adapter. The mixture was heated within 15 minutes by stirring at 160°C–165°C in silicon oil bath and then the temperature of the system was lowered to 70°C. The mixture was stirred for half an hour at 70°C to get the prepolymer. Nitrogen was vented throughout the above procedures. The prepolymer was postpolymerized at 50°C and 700°C with and without vacuum for a predetermined time from 1 day to 3 weeks depending on the temperature to achieve the nanosized poly organic acid. Nitrogen was introduced into the reaction system before the polymer was taken out from the reaction system.

The surface morphology of BCc1 was characterized using scanning electron microscopy in Razi Metallurgical Research Center.

High-resolution transmission electron microscopy images of BCc1 were captured using a transmission electron microscope in the University of Tehran Science and Technology Park.

The functional groups of BCc1 were characterized by IR spectroscopy in the 400–4,000 cm^{-1} range in the University of Shahid Beheshti.

According to a previous study,² complexometric titration was performed to verify the chelating property of BCc1.

Cytotoxicity of BCc1

Cell viability was measured by MTT assay (Sigma-Aldrich Co.). Briefly, MEFs and MCF-7 cells were seeded onto 96-well plates in triplicate wells and grown overnight in 100 μL medium. Then, the cells were incubated with fresh medium containing serial concentrations (0–1,000 $\mu\text{g}/\text{mL}$) of BCc1 for 24 hours and 48 hours. Afterward, the cells were incubated with 0.25 mg MTT/mL (final concentration) for 2 hours at 37°C, and the reaction was stopped by the addition of dimethyl sulfoxide. The formazan dye crystals were solubilized, and the absorbance was measured using a microplate reader at a test wavelength of 570 nm and a reference wavelength of 630 nm.

Evaluation of BCc1 LD50

Standard tests were carried out for assessing the median lethal dose (LD50) according to the guidelines of the Organization for Economic Co-operation and Development (guideline 420)

in the School of Pharmacy at Tehran University of Medical Sciences.

Flow cytometry analysis of CD44 and CD24 protein expression

MCF-7 cells were cultured in a medium containing 10 $\mu\text{g}/\text{mL}$ of BCc1 for 72 hours. Choosing this concentration of BCc1 was based on the results of cell toxicity test. A total of 1×10^6 cells were laid into microtubes with 100 μL phosphate-buffered saline (PBS) and stained with monoclonal antibodies against human CD44 Phycoerythrin (PE), CD24 (PE), and their respective isotype controls at 4°C in the dark for 30 minutes. The labeled cells were washed with the washing buffer and then fixed in PBS containing 1% paraformaldehyde. Isotype control is an antibody of the same isotype as a primary antibody with no relevant specificity to the target antigen. Isotype controls are used as negative controls to help differentiate nonspecific background signal from specific antibody signal. WinMDI 2.8 software was used to create the histograms.

Apoptosis assay and cell cycle analysis

According to the manufacturer's protocol, annexin V apoptosis assay was performed to investigate the cell death mechanism in MCF-7 cells. Cells were incubated with 10 $\mu\text{g}/\text{mL}$ of BCc1 for 48 hours. Choosing the concentration of BCc1 was based on the results of cell toxicity test. Afterward, the cells were washed with PBS (1 \times) and subsequently stained with fluorescein isothiocyanate, annexin V, and propidium iodide.²⁶ Cells were harvested with 3.5 mM EDTA–PBS buffer, fixed with 70% ethanol for at least 1 hour at 4°C, treated with 20 $\mu\text{g}/\text{mL}$ RNase A for 30 minutes, and stained with 60 $\mu\text{g}/\text{mL}$ propidium iodide for DNA content, and the cell cycle status was analyzed with the FACSCalibur cytometer.²⁷ WinMDI 2.8 software was used to create the density plot.

Measurement of BCc1 cell protection capacity against H_2O_2 -induced oxidative injury

H_2O_2 is used in experiments for simulation of oxidative stress condition.²⁸ MEFs were plated at a density of 1×10^4 cells/well in 96-well plates in 100 μL RPMI. They were treated with several concentrations of BCc1 for 24 hours and then incubated with 150 μM of H_2O_2 for 1 hour as test groups. For control group, the cells were cultured without treatment with BCc1 or H_2O_2 (as negative control) or treated merely with H_2O_2 for 1 hour (as positive control). Afterward, the cell viability was measured using the conventional MTT reduction assay.

In vivo studies and tumor creation

According to the method described by Langroudi et al,²⁹ spontaneously adenocarcinoma breast tumor-bearing mice were supplied. Fifteen days after transplantation, when the tumor size reached to $\sim 500 \text{ mm}^3$, 24 tumor-bearing mice were randomly divided into four BCc1-treated and control groups, each consisting of six mice: low-dose group (0.4 mg/kg), medium-dose group (10 mg/kg), high-dose group (20 mg/kg), and control group (received distilled water in the same route and volume). BCc1 was dissolved in distilled water and injected intraperitoneally once a day. The tumor volume was measured daily using a digital caliper (Mitutoyo, Japan) and the following formula: $V=1/6 (\pi LWD)$,³⁰ where L = length, W = width, and D = depth.

Survival study

Tumor transplantation was carried out as described earlier. After 15 days, when the tumor size of each mouse reached $\sim 500 \text{ mm}^3$, 16 tumor-bearing mice were randomly divided into four BCc1-treated and control groups: control group ($n=4$), low-dose group (0.1 mg/kg, $n=4$), medium-dose group (0.4 mg/kg, $n=4$), and high-dose group (1 mg/kg, $n=4$). New doses were calculated based on the results of the tumor growth study. The tumor sizes were measured up to 53 days post transplantation. BCc1 was administered via intraperitoneal (IP) injection once a day. At the end of life, each mouse was dissected and lungs and liver were removed, fixed in 10% paraformaldehyde, and were stained with H&E stain for detection of metastasis.

Histological analysis

The lungs and liver were removed and fixed in 10% formalin solution and embedded in paraffin. The paraffin-embedded

4 μm sections were stained with H&E and examined with an Olympus B51 microscope, and images were captured using the DP72 camera.

Evaluation of hematological parameters

To evaluate the effect of nanocomplex on hematologic indices, 8-week-old mice were divided into three groups ($n=4$). For 23 days, two groups of mice were IP injected with BCc1, one group with 0.1 mg/kg of BCc1 and the other with 0.4 mg/kg once a day. The control group received distilled water in the same route and volume. On day 0 and day 23, blood was drawn from the retro-orbital sinus. Red blood cells and hemoglobin determination was evaluated using an automated blood analyzer.

Statistical analysis

Each experiment was performed in duplicate or triplicate. Statistical analysis of the data was performed using the IBM SPSS Statistics 19 software. The average of data was analyzed by analysis of variance for each experiment. A P -value of 0.05 was considered to be statistically significant. Survival analysis was performed by the Kaplan–Meier method.

Results

BCc1 characteristics

Analysis of the images of BCc1 indicated that the size of the nanocomplex was $\sim 45\text{--}47 \text{ nm}$ (Figure 1A and B). The IR spectrum analysis clearly demonstrated that the BCc1 nanocomplex is an organic-hydrocarbon structure that possessed the C=O (reflecting chelating capacity), OH, and NH groups (Figure 2A) based on the available graph.

The results showed that the elevated concentrations of BCc1 co-occurred with a decrease in iron absorption

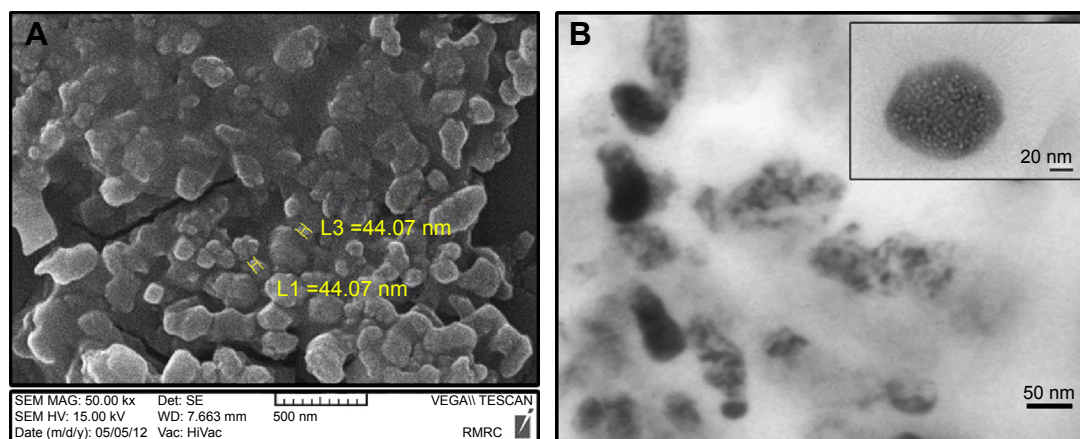


Figure 1 (A) SEM image and (B) HRTEM image of BCc1.

Note: Scale of **A** is 500 nm and two yellow particles are 44 nm.

Abbreviations: SEM, scanning electron microscopy; HRTEM, high-resolution transmission electron microscopy.

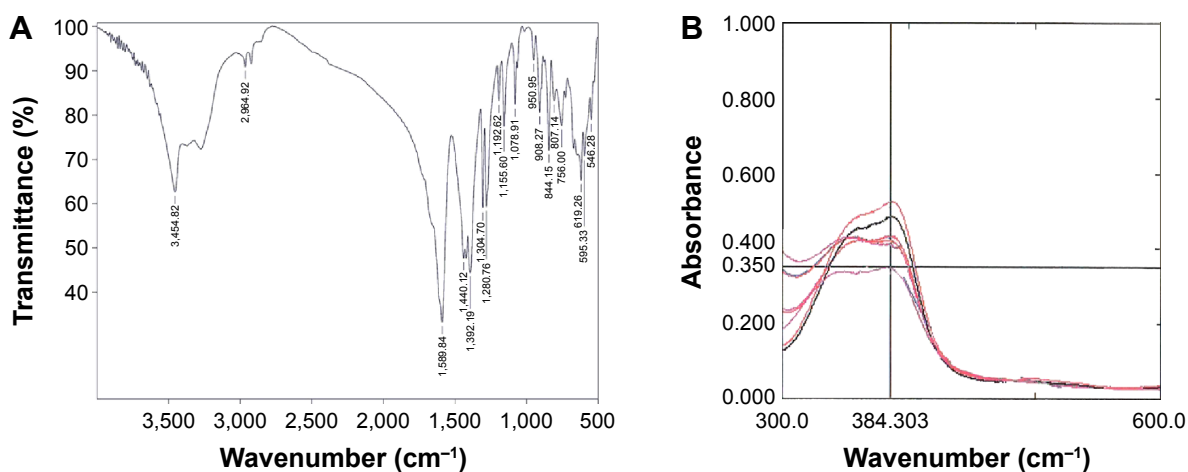


Figure 2 Infrared spectrum analysis (A) and complexometric titration (B).

spectrum, which was an indicator of iron chelation (Figure 2B).

BCcI induced cell death in malignant cells

The results showed that after 24 hours and 48 hours, BCcI cell toxicity was greater for cancer cells than MEFs. BCcI nanocomplex was a proliferation inhibitor of cancer cells, where the same concentration did not affect the viability of healthy cells. For example, the 24 hours treatment with 100 µg/mL of BCcI was significantly toxic for MCF-7 cells ($P < 0.05$) and had decreased the cell viability to 37%, while only 14% reduction in the viability of MEFs in this concentration of BCcI was observed. The viability of MEFs after 24 hours treatment with BCcI at concentrations of 1,000 µg/mL, 100 µg/mL, 10 µg/mL, 1 µg/mL, and 0.1 µg/mL was, respectively, 30%, 96%, 91%, 90%, and 100%, and thus in the concentration of 1,000 µg/mL, the

cell viability decreased significantly ($P < 0.05$), while the cell viability of MCF-7 at the same concentrations was 33%, 54%, 85%, 96%, and 85%, respectively, and thus in several concentrations, the cell viability decreased significantly ($P < 0.05$). The viability of MEFs treated for 48 hours with the above concentrations was 9%, 81%, 94%, 98%, and 100%, while the viability of MCF-7 cells at concentrations of 1,000 µg/mL, 100 µg/mL, and 10 µg/mL was significantly ($P < 0.05$) cut down to 5%, 30%, and 41% (Figure 3A and B). According to the IC₅₀ values (Table 1), BCcI has more anti-proliferative activity in neoplastic cells.

BCcI cell protection against H₂O₂-induced oxidative injury

The “Results” section showed that cell viability increased significantly in all groups treated with BCcI and at the optimum dose. It even increased up to 90% in comparison

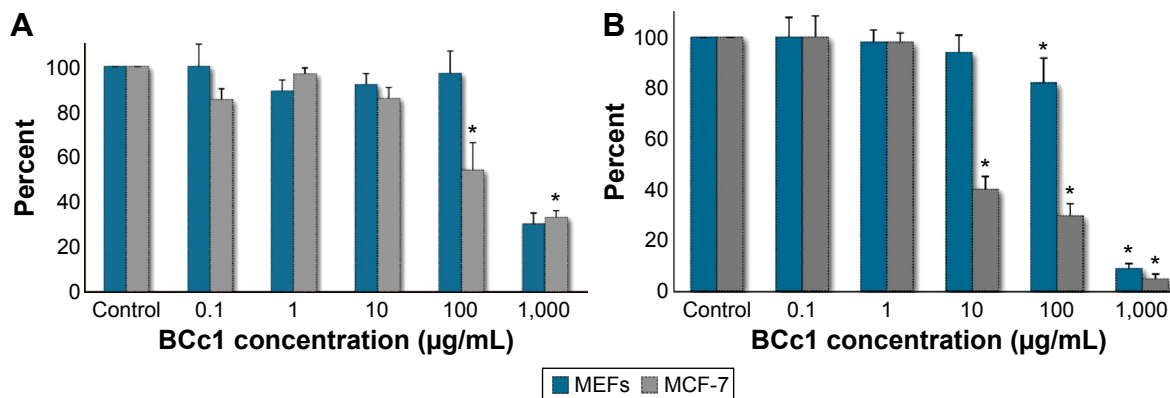


Figure 3 BCcI cell toxicity in malignant and normal cells after 24 hours (A) and 48 hours (B).

Note: Significant differences in the control cells have been specified by a single asterisk (*), meaning P -value ≤ 0.05 .

Abbreviation: MEFs, mice embryonic fibroblasts.

Table 1 IC₅₀ values in neoplastic and normal cells

	MEFs	MCF-7
24 hours	1,179±105	869±85
48 hours	705±50	493±75

Notes: Each IC₅₀ value (given in µg/mL) is the mean ± SEM of at least three experiments performed. The cells were incubated in the presence of different concentrations of BCc1 for 24 hours or 48 hours at 37°C. After this incubation period, cellular proliferation was determined by the MTT assay.

Abbreviations: IC₅₀, half maximal inhibitory concentration; MEFs, mouse embryonic fibroblasts; SEM, standard error of the mean.

to the positive control group ($P<0.05$). This nanocomplex, even in high doses (100 µg/mL), used in this test was actually able to protect cell viability against H₂O₂. The viability of these cells increased to 30% compared with control cells ($P<0.05$), while the viability of cancer cells ($P<0.05$) was significantly reduced by this dose ($P<0.05$) (Figure 4).

BCc1 is low toxic in vivo

BCc1 toxicity report showed that IP LD50 (for mouse) of this nanocomplex is 109.17 mg/kg (Table 2).

BCc1 decreased CD44 expression

MCF-7 cells were treated with BCc1 for 72 hours. Flow cytometry results showed that CD24 expression in control and BCc1-treated cells was 34% and 83%, respectively, and the expression of CD44 was 21% and 8%, respectively (Figure 5). According to the result, BCc1 decreased CD44 expression significantly ($P<0.05$).

BCc1 induced apoptosis and cell cycle arrest in MCF-7 cells

The treatment of MCF-7 cells with BCc1 showed significant induction of apoptosis in breast cancer lines. The dosage of

10 µg/mL of this nanocomplex could decrease viable MCF-7 cells and increase the percent of cells that were in early and late apoptosis and necrosis compared to control (Figure 6). The percentage of G1 cells increased from 59% to 70% with 10 µg/mL BCc1 after 48 hours. The nanocomplex decreased the percentage of S and G2/M cells from 15% and 26% to 12% and 18%, respectively (Figure 7).

BCc1 decreased the rate of tumor growth

The tumor growth rate was reduced by BCc1 in all three administered doses. The decrease seen in the lowest dose was obvious. At the end of day 23 of injection, the tumor sizes in the control group were, respectively, 40%, 25%, and 23% larger than the low-, medium-, and high-dose groups. On day 1, the tumor sizes in the control group, the low-dose group, the medium-dose group, and the high-dose group were 13.6-, 8-, 10.8-, and 11-fold, respectively (Figure 8).

BCc1 improves survival in mice with adenocarcinoma breast tumor

First, second, and third deaths were related to the control mice on 53 days, 60 days, and 66 days, respectively, after transplantation. At the same time, all mice in the treated group were alive. The last death of the control group occurred on day 75. Mice in the low-dose group died on days 72 and 74, and the mice in the high-dose group died on days 73, 75, and 76. Mice in the medium-dose group died on days 83, 85, 91, and 105 after transplantation. By calculating the mean survival days of mice, the lifetime in low-, medium-, and high-dose groups was 1.15-, 1.44-, and 1.17-fold, respectively, greater than the control group. In this manner, the

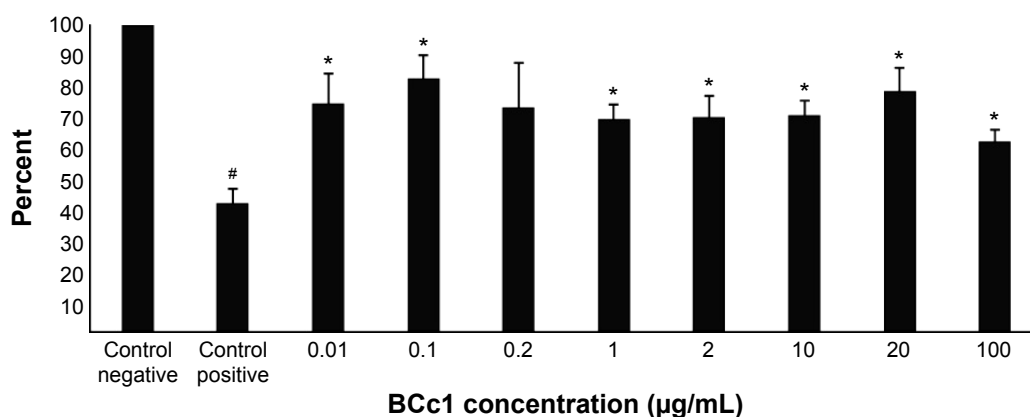


Figure 4 The protection of MEF cells from H₂O₂-induced oxidative toxicity by BCc1.

Notes: Significant differences in the H₂O₂-treated cells have been specified by a single asterisk (*), meaning P -value ≤ 0.05 . Significant differences in the control cells have been specified by a single hash (#), meaning P -value ≤ 0.05 .

Abbreviation: MEF, mice embryonic fibroblast.

Table 2 BCcI toxicity report

Group	Dose (mg/kg), IP injection	No of animals died after 24 hours	No of animals died after 48 hours	No of animals died after 72 hours	Total dead mice
1	2,000	6	0	0	6
2	1,000	6	0	0	6
3	500	6	0	0	6
4	300	6	0	0	6
5	200	6	0	0	6
6	100	2	0	0	2
7	80	1	0	0	1
8	60	0	0	0	0
9	50	0	0	0	0

Note: Intraperitoneal LD50 (mouse) – 109.17 mg/kg.

Abbreviation: IP, intraperitoneal.

medium-dose group had a 44% increased life span compared with the control mice (Figure 9).

BCcI had no negative effect on hematological indices

The evaluation of hematological indices in the two groups of mice treated by IP injection of BCcI showed that the nano-complex had no negative effect on hematological parameters (Figure 10).

BCcI prevents metastasis

In serial sections examined, two mice of the control group showed clumps of metastatic cells in the parenchyma of

liver, while none of the treated cases showed metastasis. Lung metastasis was seen in one mouse of all groups except high-dose-treated group in which none of them showed tumor cells. In some of the liver tissues, there was a prominent inflammatory cell infiltration, including neutrophils in spite of the absence of metastatic tumor. There were also prominent megakaryocytes in the sinusoids in some liver samples without predilection to any group (Figure 11).

Discussion

Considering the complex nature, drug resistance, and the intelligence of cancer cells, achieving a multifunctional cancer

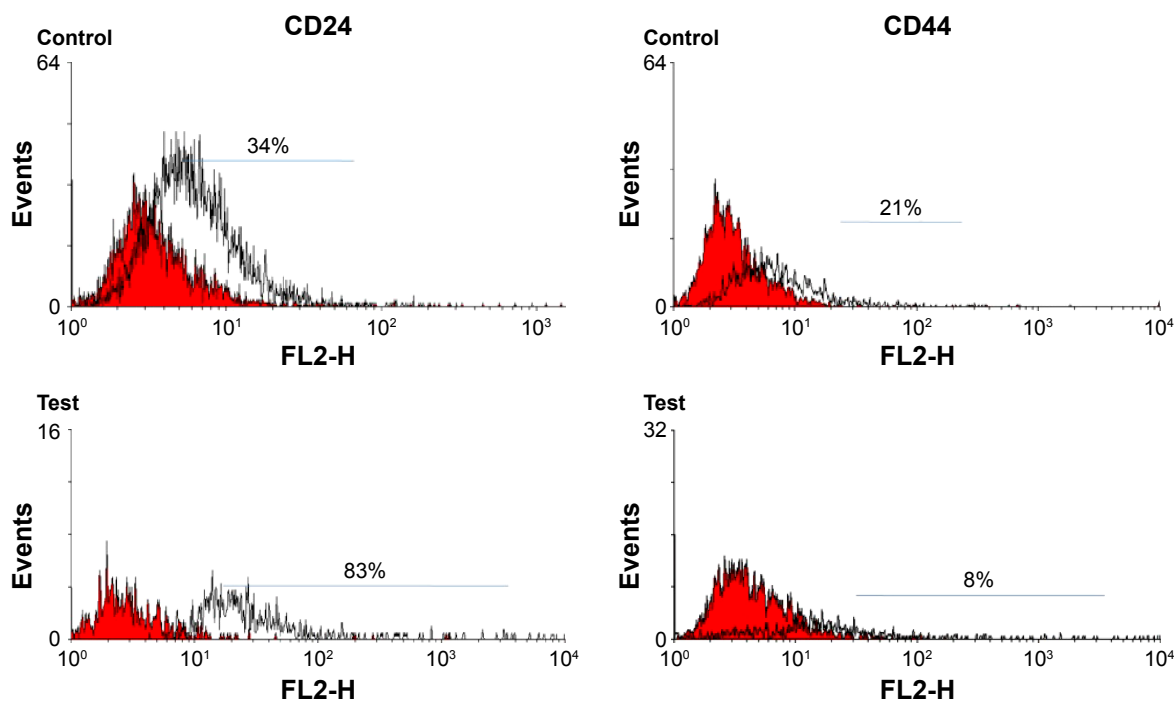


Figure 5 Expression of cell markers CD44 and CD24 in MCF-7 cell line.

Note: The histogram outlined by a black line represents positive staining for CD44 and CD24, and color-filled histograms show negative control stained with matched isotype antibody.

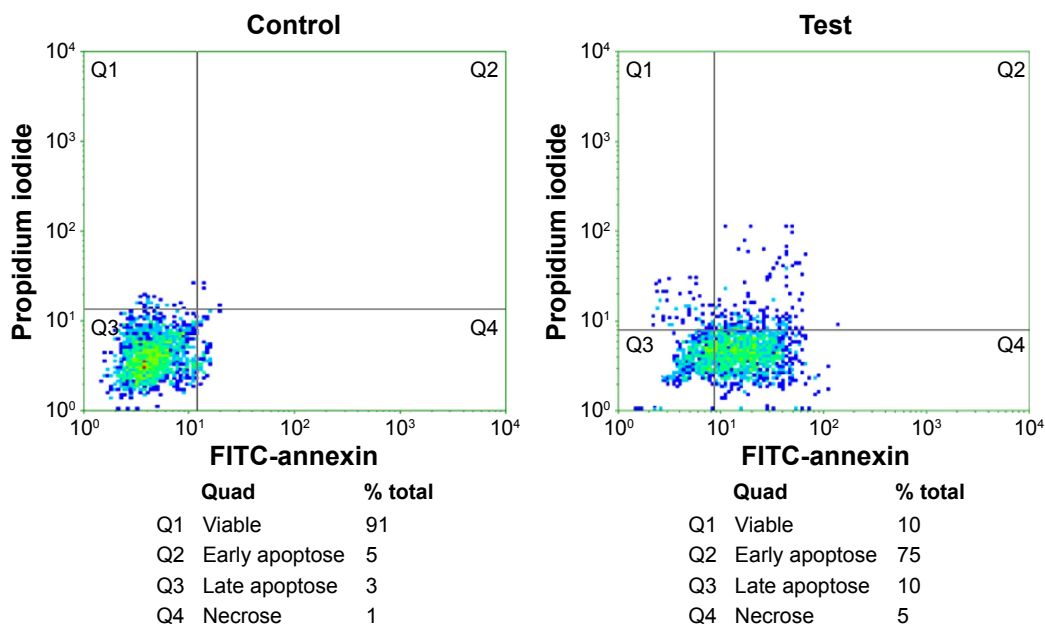


Figure 6 Flow cytometry analysis in the control and test after annexin and PI staining. **Abbreviations:** PI, propidium iodide; FITC, fluorescein isothiocyanate.

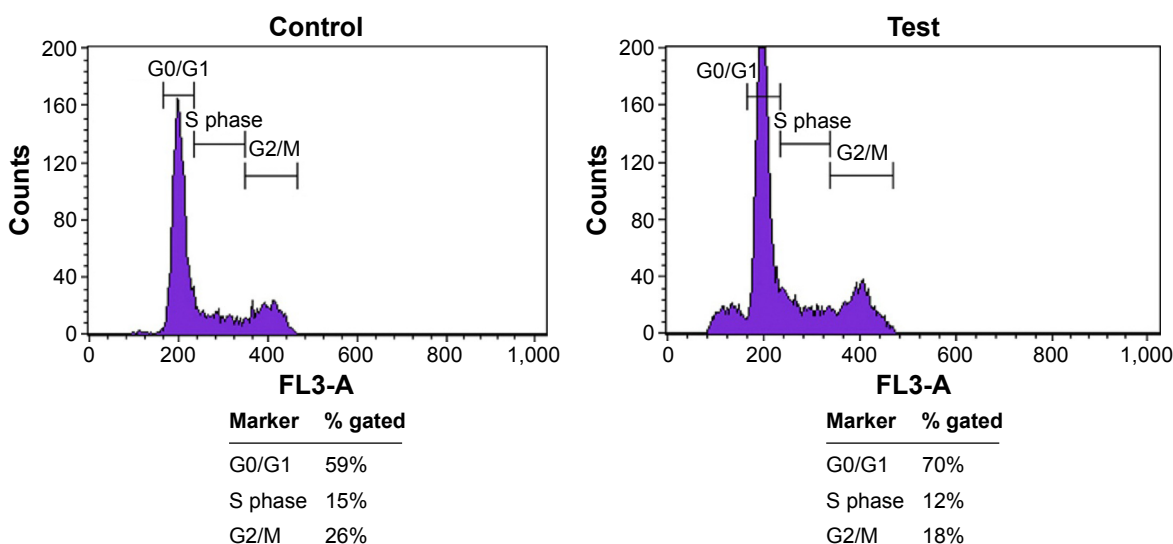


Figure 7 Flow cytometry analysis in the control and test for cell cycle analysis.

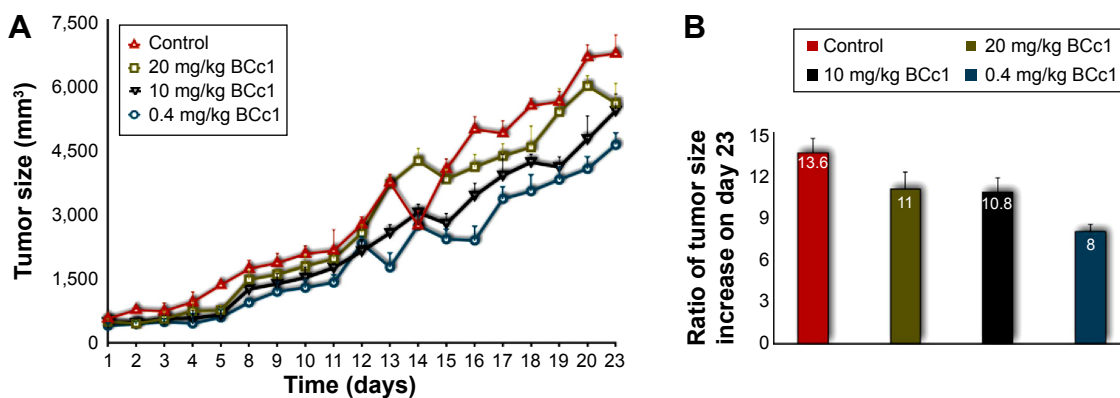


Figure 8 BCcI tumor suppressing effect (A). Ratio of tumor size on the day 23 in relation to day 1 in the control and test groups (B).

Notes: The tumor size from each group at the end of the experiment (day 23) was divided over the tumor size from each group in the beginning of the treatment (day 1) to demonstrate the efficacy of the nanocomplex in controlling tumor growth by using mathematical logic.

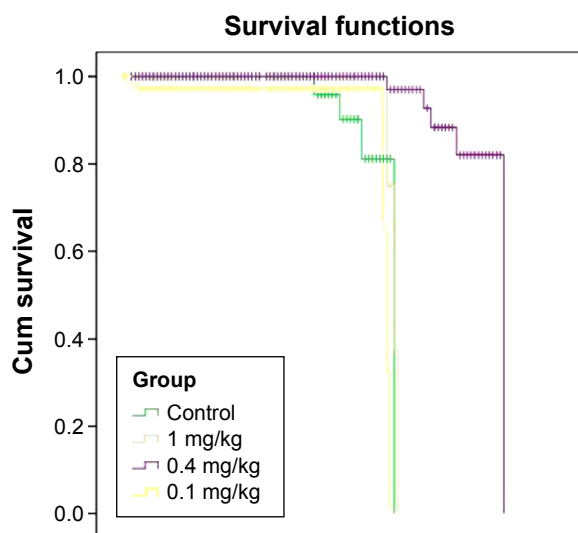


Figure 9 Survival diagrams of the control and test groups.

cell-selective agent is necessary.^{31,32} As the first synthetic nanocomplex is designed based on the nanochelating technology for cancer treatment, the present study showed that BCc1 has high potentials to induce therapeutic behavior. BCc1 was able to induce apoptosis and increased the percent of cells that were arrested in the G1 phase. The studies by Recalcati et al, Gazitt et al, and Gao et al have shown that exposure to iron chelators results in a G1/S arrest via decrease in p21CIP1/WAF1 protein expression and cyclin D inhibition.^{18,33,34} In addition, multiple reports have shown that iron chelation increases p53 transcription, translation, and DNA-binding affinity, resulting in G1/S cell cycle arrest

and/or apoptosis.³⁵⁻³⁷ Thus, it is possible that iron chelation is one of the BCc1 antineoplastic mechanisms that induces cell cycle arrest and apoptosis. Evaluations of mice bearing adenoma carcinoma of the breast revealed that BCc1 was able to increase the survival rates and decreased metastasis and the rate of tumor growth. Several studies have shown that NDRG1 expression is induced by iron chelators, which inhibit tumor growth, angiogenesis, and metastasis. On the other hand, the results of this study have revealed that BCc1 is able to effectively reduce CD44 and increase CD24 expression in cancer cell line. CD44 is considered as a potential cancer stem cell marker in the majority of cancers.³⁸ It is capable of promoting tumorigenic signals through a variety of major signaling networks. In many cancers, CD44 plays a major role in the initiation, metastasis, and promotion of tumor genesis.^{21,39-41} Considering the role of CD44 and CD24 markers in tumor invasion and metastasis, the other mechanism of BCc1 antineoplastic function is possibly via such modifications.^{42,43}

It should be noted that besides the potential beneficial use of nanoparticles for cancer therapy, the safety of nanoparticles is attracting the attention of the US Food and Drug Administration, and also Environmental Protection Agency, which is starting to look into the regulation of nanotechnology. Several studies have demonstrated that nanoparticles induce the production of reactive oxygen species and oxidative stress.^{44,45} Yang et al⁴⁶ demonstrated in their study that oxidative stress is a key route in inducing the cytotoxicity of nanoparticles. On the other hand, studies have shown that neutral organic coating increases nanomaterial biocompatibility.^{47,48}

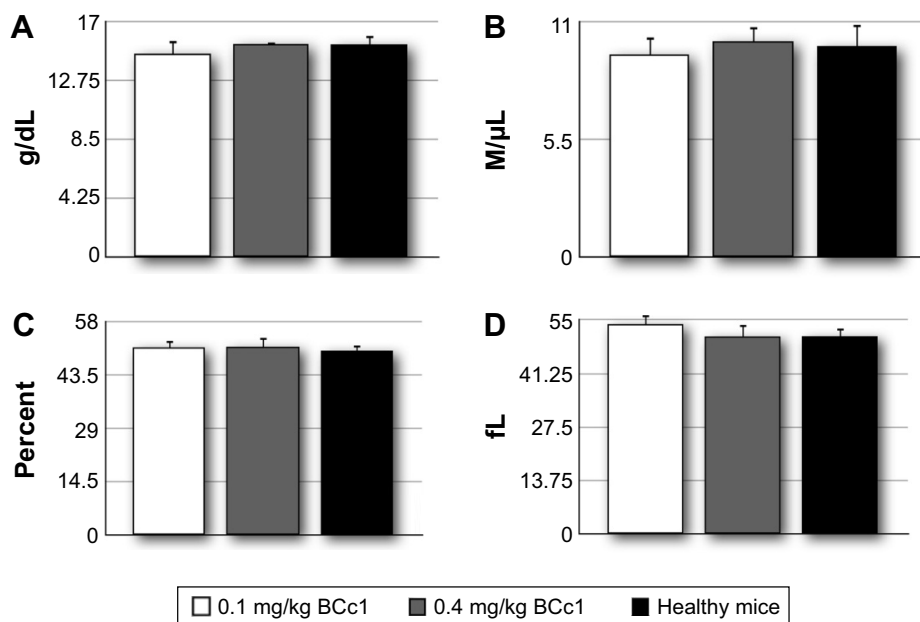


Figure 10 The average amounts for Hb concentration (A), RBC count (B), HCT (C), and MCV (D).
Abbreviations: Hb, hemoglobin; RBC, red blood cell; HCT, hematocrit; MCV, mean cell volume.

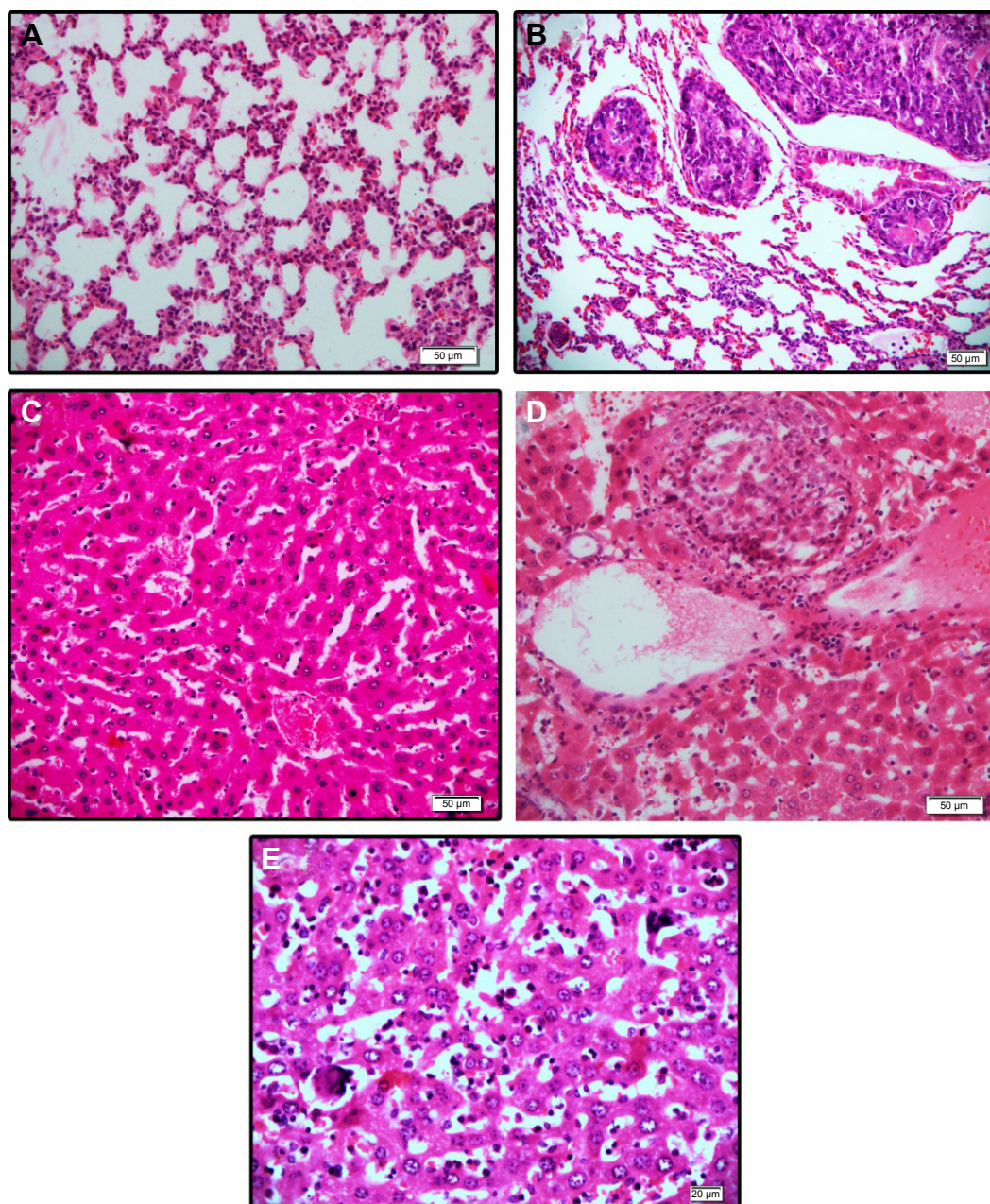


Figure 11 Hematoxylin and eosin staining of (A) normal lung tissue, (B) clumps of metastatic tumor cells, (C) normal liver tissue, (D) clumps of metastatic cells, and (E) the megakaryocyte within the liver sinusoids.

Our *in vitro* experiments showed that the lethal concentrations of BCc1 for breast cancer cell line are not toxic for healthy MEF cells. In addition, the IP LD50 of BCc1 has been reported to be 109 mg/kg. However, this study has confirmed that the optimum dosage is less than (at least 109-fold less than the determined LD50) or equal to 1 mg/kg. Also, BCc1 has had no adverse effects on hemoglobin and red blood cell levels. In addition, BCc1 like previous nanochelation-based structures, Msc1, Pac, Pas, and Paf)^{10,11} has protected cells against H₂O₂-mediated

oxidative stress, and also IR spectrum analysis has clearly demonstrated that BCc1 is an organic-hydrocarbon structure. These characters positively affect the nanocomplex biocompatibility.

Conclusion

In conclusion, the mentioned properties of BCc1, such as having synthetic organic structure, low normal cell toxicity, protecting cell viability against H₂O₂-mediated oxidative stress, decreasing CD44 expression, G1 arrest in the cell

cycle of cancer cell lines, decreasing tumor growth rate and liver metastasis, and increased survival rate, are all gathered in the BCc1 structure.

The solidarity of the mentioned results along with the modern technology by which nanocomplex has synthesized shows that BCc1 has the potential to evaluate complementary studies as an agent that induces therapeutic behavior in clinical trials of cancer disease.

Acknowledgments

This work was supported by the Department of Research and Development in the Sodour Ahrar Shargh Co and Cancer Research Center, Shahid Beheshti University of Medical Sciences, Tehran, Iran. We express our gratitude for Dr ZM Hassan (Tarbiat Modares University, Tehran, Iran) guidance. Special thanks to Dr Samira Mohammadi-Yeganeh (Shahid Beheshti University, Tehran, Iran) and Fakhrosadat Nasiri (Sodour Ahrar Shargh Co) for their assistance in this project.

Disclosure

MHN is the owner of Nanochelating Technology and executive manager and chairman of Management Board of Sodour Ahrar Shargh Co., Tehran, Iran. The authors report no other conflicts of interest in this work.

References

- Gebel E. *Cancer Deaths Declining in Developed Countries*. USA: International Organizations Coordinating Research Efforts; 2008. Available from <http://iipdigital.usembassy.gov/st/english/article/2008/06/20080625175712abretnuh0.8982965.html#axzz3pp2fHsCm>. Accessed on Oct 28, 2015.
- Shafi MA, Bresalier RS. The gastrointestinal complications of oncologic therapy. *Gastroenterol Clin North Am*. 2010;39:629–647.
- Sanches Junior JA, Brandt HR, Moure ER, Pereira GL, Criado PR. Adverse mucocutaneous reactions to chemotherapeutic agents: part I. *An Bras Dermatol*. 2010;85:425–437.
- Rebucci M, Michiels C. Molecular aspects of cancer cell resistance to chemotherapy. *Biochem Pharmacol*. 2013;85:1219–1226.
- Szebeni J. [Nanomedicine: application of nanotechnology in medicine. Opportunities in neuropsychiatry]. *Neuropsychopharmacol Hung*. 2011;13:15–24. Hungarian.
- Xu J, Ma J, Yang G. [Differentiation of human leukemia cell (HL-60) induced by *Sophora flavescens* ait. Decoction]. *Zhongguo Zhong Yao Za Zhi*. 1990;15(625–626):641. Chinese.
- Luo C, Sun J, Sun B, He Z. Prodrug-based nanoparticulate drug delivery strategies for cancer therapy. *Trends Pharmacol Sci*. 2014;35:556–566.
- Sanna V, Pala N, Sechi M. Targeted therapy using nanotechnology: focus on cancer. *Int J Nanomedicine*. 2014;9:467–483.
- Fakharzadeh S, Kalanaky S, Hafizi M, et al. The new nano-complex, Hep-c, improves the immunogenicity of the hepatitis B vaccine. *Vaccine*. 2013;31(22):2591–2597.
- Fakharzadeh S, Sahraian MA, Hafizi M, et al. The therapeutic effects of MSc1 nano-complex, synthesized by nanochelating technology, on experimental autoimmune encephalomyelitis C57/BL6 mice. *Int J Nanomedicine*. 2014;9:3841–3853.
- Maghsoudi A, Fakharzadeh S, Hafizi M, et al. Neuroprotective effects of three different sizes nanochelating based nano complexes in MPP(+) induced neurotoxicity. *Apoptosis*. 2015;20:298–309.
- Zacharski LR, Chow BK, Howes PS, et al. Decreased cancer risk after iron reduction in patients with peripheral arterial disease: results from a randomized trial. *J Natl Cancer Inst*. 2008;100:996–1002.
- Toyokuni S. Role of iron in carcinogenesis: cancer as a ferrototoxic disease. *Cancer Sci*. 2009;100:9–16.
- Aye Y, Li M, Long MJ, Weiss RS. Ribonucleotide reductase and cancer: biological mechanisms and targeted therapies. *Oncogene*. 2015;34:2011–2021.
- Siriwardana G, Seligman PA. Iron depletion results in Src kinase inhibition with associated cell cycle arrest in neuroblastoma cells. *Physiol Rep*. 2015;3:e12341.
- Hosoi F, Izumi H, Kawahara A, et al. N-myc downstream regulated gene 1/Cap43 suppresses tumor growth and angiogenesis of pancreatic cancer through attenuation of inhibitor of kappaB kinase beta expression. *Cancer Res*. 2009;69:4983–4991.
- Furukawa T, Naitoh Y, Kohno H, Tokunaga R, Taketani S. Iron deprivation decreases ribonucleotide reductase activity and DNA synthesis. *Life Sci*. 1992;50:2059–2065.
- Gao J, Richardson DR. The potential of iron chelators of the pyridoxal isonicotinoyl hydrazone class as effective antiproliferative agents, IV: the mechanisms involved in inhibiting cell-cycle progression. *Blood*. 2001;98:842–850.
- Maruyama Y, Ono M, Kawahara A, et al. Tumor growth suppression in pancreatic cancer by a putative metastasis suppressor gene Cap43/NDRG1/Drg-1 through modulation of angiogenesis. *Cancer Res*. 2006;66:6233–6242.
- de Beça FF, Caetano P, Gerhard R, et al. Cancer stem cells markers CD44, CD24 and ALDH1 in breast cancer special histological types. *J Clin Pathol*. 2013;66:187–191.
- Godar S, Ince TA, Bell GW, et al. Growth-inhibitory and tumor-suppressive functions of p53 depend on its repression of CD44 expression. *Cell*. 2008;134:62–73.
- Reuter S, Gupta SC, Chaturvedi MM, Aggarwal BB. Oxidative stress, inflammation, and cancer: how are they linked? *Free Radic Biol Med*. 2010;49:1603–1616.
- Sosa V, Moline T, Somoza R, Paciucci R, Kondoh H, ME LL. Oxidative stress and cancer: an overview. *Ageing Res Rev*. 2013;12:376–390.
- Wu FJ, Xue Y, Liu XF, et al. The protective effect of eicosapentaenoic acid-enriched phospholipids from sea cucumber *Cucumaria frondosa* on oxidative stress in PC12 cells and SAMP8 mice. *Neurochem Int*. 2014;64:9–17.
- Nazaran MH. Chelate compounds. Google Patents US8288587; 2012.
- Riccardi C, Nicoletti I. Analysis of apoptosis by propidium iodide staining and flow cytometry. *Nat Protoc*. 2006;1:1458–1461.
- Wang XW, Zhan Q, Coursen JD, et al. GADD45 induction of a G2/M cell cycle checkpoint. *Proc Natl Acad Sci U S A*. 1999;96:3706–3711.
- Si CL, Shen T, Jiang YY, et al. Antioxidant properties and neuroprotective effects of isocampneoside II on hydrogen peroxide-induced oxidative injury in PC12 cells. *Food Chem Toxicol*. 2013;59:145–152.
- Langroudi L, Hassan ZM, Ebtakar M, Mahdavi M, Pakravan N, Noori S. A comparison of low-dose cyclophosphamide treatment with artemisinin treatment in reducing the number of regulatory T cells in murine breast cancer model. *Int Immunopharmacol*. 2010;10(9):1055–1061. doi: 10.1016/j.intimp.2010.06.005. Epub 2010 July 2.
- Liu M, Bryant MS, Chen J, et al. Antitumor activity of SCH 66336, an orally bioavailable tricyclic inhibitor of farnesyl protein transferase, in human tumor xenograft models and wap-ras transgenic mice. *Cancer Res*. 1998;58:4947–4956.
- Gottesman MM. Mechanisms of cancer drug resistance. *Annu Rev Med*. 2002;53:615–627.
- Apisarnthanarax N, Duvic M. Dermatologic Complications of Cancer Chemotherapy. In: Bast RC Jr, Kufe DW, Pollock RE, et al., editors. *Holland-Frei Cancer Medicine*. 5th edition. Hamilton (ON): BC Decker; 2000:144.

33. Recalcati S, Alberghini A, Campanella A, et al. Iron regulatory proteins 1 and 2 in human monocytes, macrophages and duodenum: expression and regulation in hereditary hemochromatosis and iron deficiency. *Haematologica*. 2006;91:303–310.
34. Gazitt Y, Reddy SV, Alcantara O, Yang J, Boldt DH. A new molecular role for iron in regulation of cell cycling and differentiation of HL-60 human leukemia cells: iron is required for transcription of p21(WAF1/CIP1) in cells induced by phorbol myristate acetate. *J Cell Physiol*. 2001;187:124–135.
35. Fukuchi K, Tomoyasu S, Watanabe H, Kaetsu S, Tsuruoka N, Gomi K. Iron deprivation results in an increase in p53 expression. *Biol Chem Hoppe Seyler*. 1995;376:627–630.
36. Liang SX, Richardson DR. The effect of potent iron chelators on the regulation of p53: examination of the expression, localization and DNA-binding activity of p53 and the transactivation of WAF1. *Carcinogenesis*. 2003;24:1601–1614.
37. Saletta F, Suryo Rahmanto Y, Noulisri E, Richardson DR. Iron chelator-mediated alterations in gene expression: identification of novel iron-regulated molecules that are molecular targets of hypoxia-inducible factor-1 alpha and p53. *Mol Pharmacol*. 2010;77:443–458.
38. Du L, Wang H, He L, et al. CD44 is of functional importance for colorectal cancer stem cells. *Clin Cancer Res*. 2008;14:6751–6760.
39. Leung EL, Fiscus RR, Tung JW, et al. Non-small cell lung cancer cells expressing CD44 are enriched for stem cell-like properties. *PLoS One*. 2010;5:e14062.
40. Weber GF, Bronson RT, Ilagan J, Cantor H, Schmits R, Mak TW. Absence of the CD44 gene prevents sarcoma metastasis. *Cancer Res*. 2002;62:2281–2286.
41. Günthert U, Hofmann M, Rudy W, et al. A new variant of glycoprotein CD44 confers metastatic potential to rat carcinoma cells. *Cell*. 1991; 65:13–24.
42. Hiraga T, Ito S, Nakamura H. Cancer stem-like cell marker CD44 promotes bone metastases by enhancing tumorigenicity, cell motility, and hyaluronan production. *Cancer Res*. 2013;73:4112–4122.
43. Shiozawa Y, Nie B, Pienta KJ, Morgan TM, Taichman RS. Cancer stem cells and their role in metastasis. *Pharmacol Ther*. 2013;138: 285–293.
44. Nel A, Xia T, Madler L, Li N. Toxic potential of materials at the nano-level. *Science*. 2006;311:622–627.
45. Lin W, Huang YW, Zhou XD, Ma Y. In vitro toxicity of silica nanoparticles in human lung cancer cells. *Toxicol Appl Pharmacol*. 2006; 217:252–259.
46. Yang H, Liu C, Yang D, Zhang H, Xi Z. Comparative study of cytotoxicity, oxidative stress and genotoxicity induced by four typical nanomaterials: the role of particle size, shape and composition. *J Appl Toxicol*. 2009;29:69–78.
47. Burns AA, Vider J, Ow H, et al. Fluorescent silica nanoparticles with efficient urinary excretion for nanomedicine. *Nano Lett*. 2009;9: 442–448.
48. Ruggiero A, Villa CH, Bander E, et al. Paradoxical glomerular filtration of carbon nanotubes. *Proc Natl Acad Sci U S A*. 2010;107: 12369–12374.

Drug Design, Development and Therapy

Publish your work in this journal

Drug Design, Development and Therapy is an international, peer-reviewed open-access journal that spans the spectrum of drug design and development through to clinical applications. Clinical outcomes, patient safety, and programs for the development and effective, safe, and sustained use of medicines are a feature of the journal, which

Submit your manuscript here: <http://www.dovepress.com/drug-design-development-and-therapy-journal>

Dovepress

has also been accepted for indexing on PubMed Central. The manuscript management system is completely online and includes a very quick and fair peer-review system, which is all easy to use. Visit <http://www.dovepress.com/testimonials.php> to read real quotes from published authors.